Progress In Electromagnetics Research, PIER 79, 75–90, 2008

PATTERN SYNTHESIS OF CONFORMAL ANTENNA ARRAY BY THE HYBRID GENETIC ALGORITHM

Z. Xu, H. Li, and Q.-Z. Liu

National Laboratory of Antennas and Microwave Technology
Xidian University
Xi'an 710071, P. R. China

J.-Y. Li

Temasek Laboratories
National University of Singapore
10 Kent Ridge Crescent, 119260, Singapore

Abstract—Desired far-field radiation patterns of 5×11 conformal antenna array are synthesized using a hybrid genetic algorithm (HGA), which combines the simplified quadratic interpolation (SQI) method and the real-coded genetic algorithm (RCGA). This hybrid genetic algorithm is shown to outperform standard genetic algorithm (GA) when used to synthesize amplitude weights of the elements to satisfy specified deep notches, nulls and average sidelobe level constraints. The HGA procedure appears to be a high effective means to compensate the mutual coupling effects on the individual element patterns for the conformal antenna array.

1. INTRODUCTION

Pattern synthesis is known as the process of choosing the parameters of an antenna array to produce desired radiation characteristics. There are a wide variety of techniques that have been developed for the synthesis of linear and planar arrays [1–6]. GA is used to thin a large linear array of uniformly excited isotropic elements to yield SLL equal to or below a fixed level, while the percentage of thinning is equal to or above a fixed value [7]. Some more complicated problems of synthesizing radiation patterns of conformal antenna array have also been considered. The least mean square error of the constrained least-squares optimization method is introduced to

synthesize the large conformal antenna arrays with constraints for the element excitation amplitudes and a phase synthesis with predefined amplitudes [8]. [9] has combined the projection method with mutual coupling compensation to obtain a sidelobe constraint pattern of the conformal antenna array especially in digital beam forming systems. A simulated annealing technique developed for circular arc arrays is presented as a method for synthesizing the radiation pattern for three-dimensional (3-D) conformal arrays in [10]. [11] describes the application of Zitler's Strength Pareto Evolutionary Algorithm II (SPEA2) to the optimization of the complex excitations for a 225 element conformal antenna array. A new method for optimizing the partitioning of conformal arrays into subarrays is also presented in [11]. Boeringer et al. demonstrate the synthesis of amplitude-only, phase-only and complex weighting for a specified far-field sidelobe envelope by the implement of a real-valued genetic algorithm that simultaneously adapts several parameters during the optimization process [12].

Compared with standard GA, this paper show the application of hybrid genetic algorithm (HGA) [13] to optimize the radiation pattern in the main operational plane of multilayer patches antennas mounted on a finite-length dielectric circular cylinder. For accurate simulation, coupling effects on the individual patterns of the array elements have been considered. It is shown that the optimal set of element excitation amplitudes can be obtained by HGA effectively for synthesizing the notched radiation patterns with given goal notch depth, nulls and sidelobe level.

2. CONFORMAL ANTENNA ARRAY THEORY

We consider an element of $A_{mn}(\theta_{mn}, \phi_{mn})$ mounted on a finite length dielectric-coated cylindrical platform, such as Fig. 1.

The far-field radiation pattern produced by $M \times N$ elements placed on the cylinder can be expressed as

$$F(\theta, \phi) = \sum_{m=1}^{M} \sum_{n=1}^{N} I_{mn} f_{mn}(\theta, \phi) \exp[j(kR_{mn} \cos \gamma_{mn} + \varphi_{mn})] \quad (1)$$

where I_{mn} is the element excitation current amplitude, φ_{mn} is the excitation current phase, and $f_{mn}(\theta, \phi)$ is the individual element pattern for A_{mn}. R_{mn} is the distance between A_{mn} and the coordinate origin o. γ_{mn} is the angle between reference direction vector $\vec{r}$ and element position vector $\vec{r}_{mn}$, and k is the free-space wavenumber.

In Fig. 1, the other relative parameters in the system of conformal

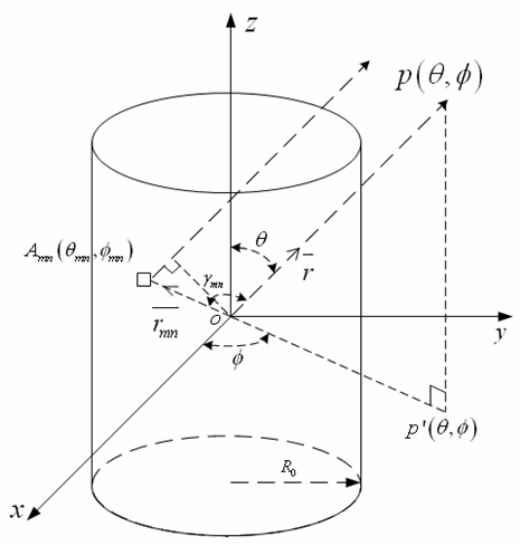

Figure 1. Illustration of element mounted on a finite length dielectric-coated cylindrical platform.

array can be expressed as follow

$$\hat{r} = \hat{x}\sin\theta\cos\phi + \hat{y}\sin\theta\sin\phi + \hat{z}\cos\theta \tag{2}$$

$$\hat{r}_{mn} = \hat{x}\sin\theta_{mn}\cos\phi_{mn} + \hat{y}\sin\theta_{mn}\sin\phi_{mn} + \hat{z}\cos\theta_{mn} \tag{3}$$

$$\begin{aligned}\cos\gamma_{mn} &= \hat{r}\cdot\hat{r}_{mn}\\ &= \sin\theta\sin\theta_{mn}\cos\phi\cos\phi_{mn} + \sin\theta\sin\theta_{mn}\sin\phi\sin\phi_{mn}\\ &\quad + \cos\theta\cos\theta_{mn}\\ &= \cos^2\left(\frac{\phi-\phi_{mn}}{2}\right)\cos(\theta-\theta_{mn})\\ &\quad + \sin^2\left(\frac{\phi-\phi_{mn}}{2}\right)\cos(\theta+\theta_{mn})\end{aligned} \tag{4}$$

$$\vec{r}_{mn} = \hat{x}A_{mn}(x) + \hat{y}A_{mn}(y) + \hat{z}A_{mn}(z) \tag{5}$$

$$\begin{aligned}R_{mn}\cos\gamma_{mn} &= \vec{r}_{mn}\cdot\hat{r}\\ &= A_{mn}(x)\sin\theta\cos\phi + A_{mn}(y)\sin\theta\sin\phi\\ &\quad + A_{mn}(z)\cos\theta\end{aligned} \tag{6}$$

$$\varphi_{mn} = -k[A_{mn}(x)\sin\theta_0\cos\phi_0 + A_{mn}(y)\sin\theta_0\sin\phi_0 + A_{mn}(z)\cos\theta_0 \tag{7}$$

where (θ_0, ϕ_0) is the desired steering angle.

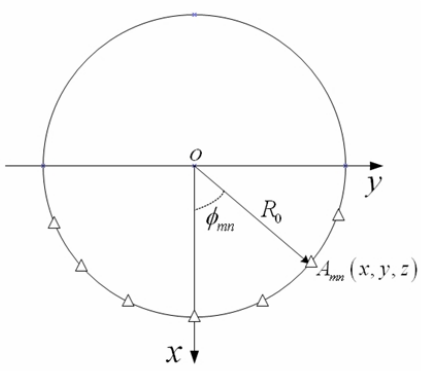

Figure 2. top-view of conformal array.

Fig. 2 shows the top-view of the conformal array, where the x coordinate of element $A_{mn}(x, y, z)$ can be written as

$$A_{mn}(x) = R_0 \cos \phi_{mn} \tag{8}$$

y and z coordinates of $A_{mn}(x, y, z)$ are expressed as follow

$$A_{mn}(y) = R_0 \sin \phi_{mn} \tag{9}$$

$$A_{mn}(z) = \frac{(M + 1 - 2m) \cdot d}{2} \tag{10}$$

Azimuthal angle

$$\phi_{mn} = \frac{(2n - 1 - N) \cdot \Delta\phi}{2} \tag{11}$$

$\Delta\phi$ represents the azimuthal angle difference between adjacent elements in the horizontal plane, d is the distance of vertical adjacent elements.

Considering above conditions, formula (1) is derived as

$$\begin{aligned} F(\theta, \phi) = & \sum_{m=1}^{M} \sum_{n=1}^{N} I_{mn} f_{mn}(\theta, \phi) \exp\{j[k(A_{mn}(x) \sin\theta \cos\phi \\ & + A_{mn}(y) \sin\theta \sin\phi) + A_{mn}(z) \cos\theta) + \varphi_{mn}]\} \end{aligned} \tag{12}$$

3. HYBRID GENETIC ALGORITHM

Hybrid genetic algorithm used in this paper combines the simplified quadratic interpolation (SQI) method and the real-coded genetic algorithm (RCGA) [13]. In RCGA, all the constraints are incorporated

into the fitness function by using the exact penalty method. The combination of an arithmetical crossover and a heuristic crossover is taken as the crossover operator. The mutation operator enhances the random search ability of the algorithm. We also adopt the ranking selection and introduce some foreign individuals into the population in order to maintain its diversity. The SQI method is used in [14] to conduct global searches. However, we integrate the SQI method into RCGA to improve its local search ability, and to make the algorithm escape from the local optima.

3.1. A Real-coded Genetic Algorithm

3.1.1. Generation of Initial Population

Vector $x = [x_1, x_2, \cdots, x_n]^\top$ is used to express an individual, which represents a solution of problem.

We generate at random *pop* uniformly distributed initial individuals $x^i(0)$, $i = 1, 2, \cdots, pop$, where *pop* denotes the population size.

3.1.2. Fitness Function

Since the problem under discussion is a minimization problem, for convenience, we stipulate that a fitness function $fit(x)$ should satisfy the following criterion: the smaller the fitness value, the better the solution. Normal format of fitness function could be written as

$$Fitness = \omega \cdot \left| 20 \cdot \log \left(\frac{1}{X_{fit}} \sum_{x \in X_{fit}} f(x) \right) - goal \right|^2 \tag{13}$$

where ω represents weight function, X_{fit} is given optimization domain, and *goal* expressed as specified target.

3.1.3. Crossover Operator

Let p_c be the crossover probability. Randomly select two parents with probability p_c: $x^1 = [x_1^1, x_2^1, \cdots, x_n^1]^\top$ and $x^2 = [x_1^2, x_2^2, \cdots, x_n^2]^\top$, and generate the offspring $y = [y_1, y_2, \cdots, y_n]^\top$according to

$$y = \begin{cases} x^1 + \Gamma(x^1 - x^2), & \text{if } fit(x^1) \le fit(x^2) \\ x^2 + \Gamma(x^2 - x^1), & \text{otherwise} \end{cases} \tag{14}$$

where $\Gamma = diag(\gamma_1, \cdots, \gamma_n)$, $\gamma_i \in (-1, 1)$, $\gamma_i \neq 0$, $i = 1, \cdots, n$.

3.1.4. Mutation Operator

Let p_m be the mutation probability, and let the best individual, an individual with minimal fitness value among all individuals generated till now, be $best = [best_1, best_2, \cdots, best_n]^\top$.

For every offspring $y = [y_1, \cdots, y_n]^\top$ such that $\|best - y\| \geq \varepsilon_1$ ($\varepsilon_1 = 10^{-4}$), randomly generate a number $rn \in [0, 1]$. If $rn < p_m$, then generate offspring $z = [z_1, \cdots, z_n]^\top$ by

$$z = best + V \cdot |c|, \tag{15}$$

where $V = diag(best_1 - y_1, \cdots, best_n - y_n)$, $c \in R^n$ is a random vector obeying an n-dimensional standard normal distribution, i.e., $c \sim [N(0, 1), \cdots, N(0, 1)]^\top$.

For every offspring $y = [y_1, \cdots, y_n]^\top$ such that $\|best - y\| < \varepsilon_1$ ($\varepsilon_1 = 10^{-4}$), we also randomly generate a number $rn \in [0, 1]$. If $rn < p_m$, then generate offspring $z = [z_1, \cdots, z_n]^\top$ by

$$z = best + \triangle v, \tag{16}$$

where $\triangle v \sim N(0, \sigma^2) = [N(0, \sigma_1^2), \cdots, N(0, \sigma_n^2)]^\top$, an n-dimensional normal distribution with mean value $0 = [0, \cdots, 0]^\top$ and deviation $\sigma^2 = [\sigma_1^2, \cdots, \sigma_n^2]^\top$.

3.1.5. Selection Operator

In order to maintain the diversity of population and avoid being trapped into local optima, we adopt the following selection strategy.

First we rank all the individuals ascendingly, consisting of those in the current population and the offspring generated by the crossover and mutation operators, according to their fitness values. Then, the best $pop - N_n$ individuals are selected, and we randomly generate N_n individuals (using the method for generating the initial population). Thus, these *pop* individuals constitute the next population. In addition, we retain the best individual of every generation.

3.1.6. Stop Criterion

If the algorithm is executed to the maximal number of generations $MaxG$, then stop. The best solution we found in the last population is then taken as the approximate global optimal solution.

3.2. A Simplified Quadratic Interpolation Method

As a local search operator, the three-point quadratic interpolation method is integrated into RCGA in order to improve its local search ability and avoid its premature convergence.

Denote three individuals by $x^a = [x_1^a, \cdots, x_n^a]^\top$, $x^b = [x_1^b, \cdots, x_n^b]^\top$, $x^c = [x_1^c, \cdots, x_n^c]^\top$, and calculate their fitness values $f_a = fit(x^a)$, $f_b = fit(x^b)$, $f_c = fit(x^c)$. Suppose that $f_a > f_b$ and $f_c > f_b$, then the approximate minimal point $\bar{x} = [\bar{x}_1, \cdots, \bar{x}_n]^\top$ derived from the three-point quadratic interpolation is expressed as follows:

$$\bar{x}_i = \frac{1}{2}\left\{\frac{[(x_i^b)^2 - (x_i^c)^2]f_a + [(x_i^c)^2 - (x_i^a)^2]f_b + [(x_i^a)^2 - (x_i^b)^2]f_c}{(x_i^b - x_i^c)f_a + (x_i^c - x_i^a)f_b + (x_i^a - x_i^b)f_c}\right\}, \quad i = 1, \cdots, n. \tag{17}$$

As is known, GA has better global search ability, while the quadratic interpolation method has powerful local search ability. Thus we integrate the quadratic interpolation method into the RCGA to form HGA, which improves the efficiency of the algorithm.

Now we can describe HGA procedure as follows.

Data. Parameter setting

Choose population size pop, crossover probability p_c, mutation probability p_m, maximal number of generations $MaxG$, and a suitable integer N_n such that $N_n < pop$.

Step 0. Initialization

Set $kk = 0$, generate randomly the initial population set $P(kk) = \{x^1(kk), \cdots, x^{pop}(kk)\}$ and compute the fitness values $fit(x^i(kk)), i = 1, 2, \cdots, pop$.

Step 1. Crossover

Step 1.1. Generate at random a number $r_1 \in [0, 1]$ and two integers $r_2, r_3 \in [1, pop]$, $r_2 \neq r_3$. If $r_1 < p_c$, then take $x^{r_2}(kk)$ and $x^{r_3}(kk)$ as two parents, execute crossover operator (14) and produce their offspring $y(kk)$.

Step 1.2. Repeat Step 1.1 pop times, produce pop_c offspring individuals, which form a trial population set denoted by $P_c(kk) = \{y^1(kk), \cdots, y^{pop_c}(kk)\}$, and compute their fitness values $fit(y^i(kk)), i = 1, 2, \cdots, pop_c$.

Step 2. Mutation

Step 2.1. For $i = 1, \cdots, pop_c$, if $\|best - y^i(kk)\| \geq \varepsilon_1$ ($\varepsilon_1 = 10^{-4}$), then generate randomly a number $rn \in [0, 1]$. If $rn < p_m$, then generate offspring $z(kk)$ by using Equ. (15). Otherwise, also

generate randomly a number $rn \in [0, 1]$. If $rn < p_m$, then generate offspring $z(kk)$ by using Equ. (16).

Step 2.2. By using Step 2.1, produce pop_m offspring individuals, which form a trial population set denoted by $P_m(kk) = \{z^1(kk), \cdots, z^{pop_m}(kk)\}$, and compute the fitness values $fit(z^i(kk)), i = 1, 2, \cdots, pop_m$.

Step 3. Local search

Step 3.1. Compare the fitness values of all the individuals, including those in the current population and all the offspring generated by the crossover and mutation operators, order ascendingly and relabel them.

Step 3.2. The three best individuals are chosen, denoted by x^b,x^a,and x^c, respectively, such that $f_b = fit(x^b) \leq f_a = fit(x^a) \leq f_c = fit(x^c)$.

Step 3.3. For some $i \in \{1, 2, \cdots, n\}$, if$(x_i^b - x_i^c)f_a + (x_i^c - x_i^a)f_b + (x_i^a - x_i^b)f_c < \varepsilon_2$ ($\varepsilon_2 = 10^{-5}$), then let $\bar{x} = x^b$, and $fit(\bar{x}) = f_b$, go to Step 3.5; Otherwise, go to Step 3.4.

Step 3.4. Calculate $\bar{x}$ by using Equ. (17), and then the fitness value $fit(\bar{x})$.

Step 3.5. If $fit(\bar{x}) < f_b$, then replace the worst solution in current population with $\bar{x}$; Otherwise, replace the worst solution in current population with x^b.

Step 4. Selection

According to the selection strategy, select *pop* individuals to constitute the next population, and retain the best individual.

Step 5. If the stopping criterion is met, then stop, and record the best individual in the last population as the approximate global optimal solution of problem. Otherwise, set $kk = kk + 1$, and go to Step 1.

Flowchart of HGA is shown in Fig. 3.

4. MODEL CONFIGURATION

The hybrid genetic algorithm presented in the previous section is applied to the case of multilayer patches antenna array mounted on a finite length dielectric-coated circular cylinder. The cylinder under consideration has a length of 7λ and a radius of 2.5λ, λ standing for the operating wavelength.

The multilayer patches antenna used in this phased array is illustrated in Fig. 4. Two perfect conductive radiation patches are

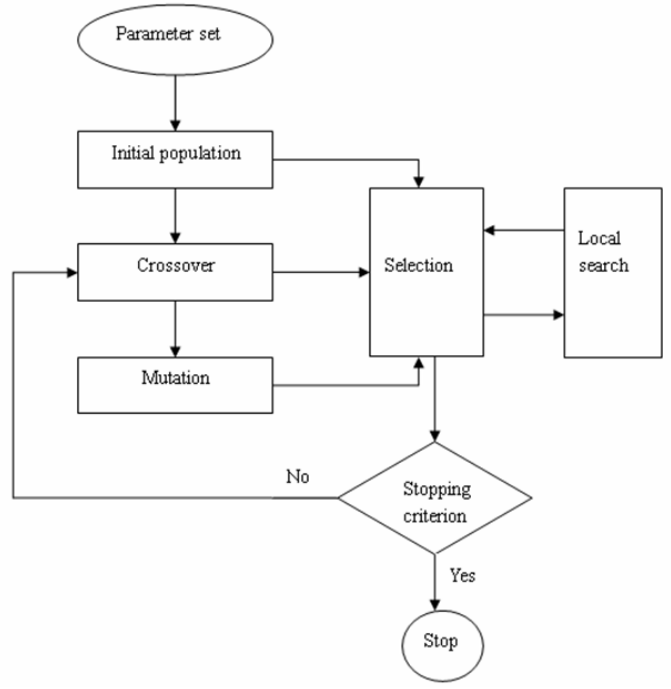

Figure 3. Flowchart of hybrid genetic algorithm (HGA).

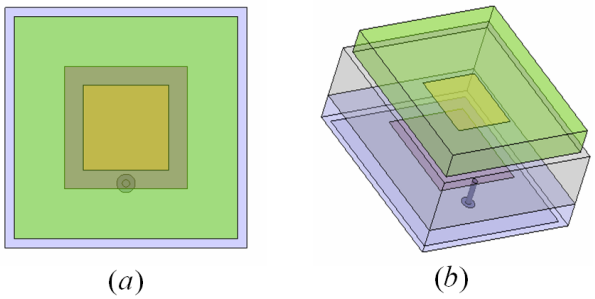

(*a*) (*b*)

Figure 4. Element illustration of multilayer patches antenna. (a) top view, (b) 3D view.

embedded into the dielectric, and the ground plane is mounted on the substrate of antenna.

Elements compose an array of 5×11 in the dimensions of $\Delta\phi = \frac{\pi}{18}$(rad) and $d = \frac{\lambda}{2}$, shown in Fig. 5. XY-plane is discussed as the main operational plane.

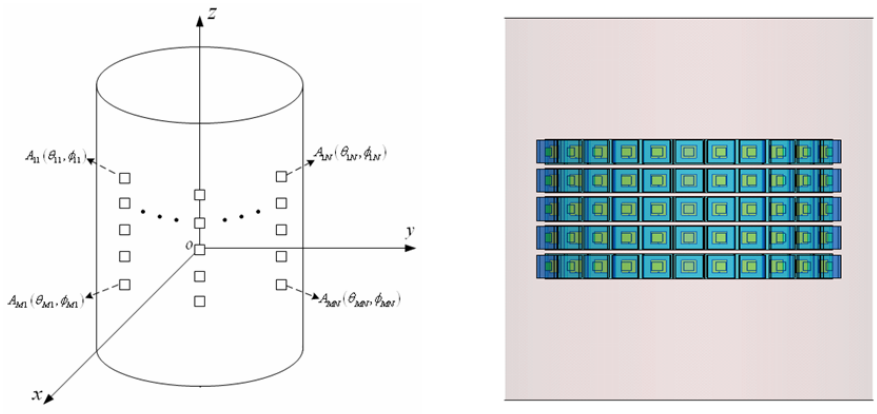

(a) (b)

Figure 5. Configuration of 5×11 conformal array.
(a) denoted elements in the array, (b) simulated model of array.

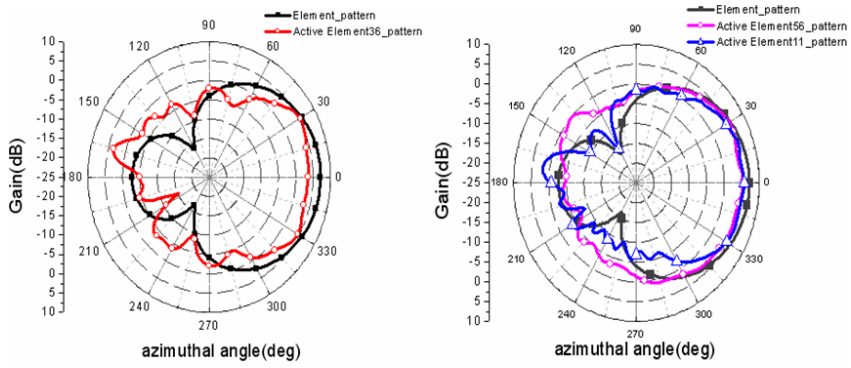

(a) (b)

Figure 6. Comparison between active element patterns and isolated element pattern. (a) active element pattern of A_{36} and isolated element pattern. (b) active element patterns of A_{11}, A_{56} and isolated element pattern.

We first seek to determine the effects of mutual coupling between elements in the antenna array. In Fig. 5, element placed at the fringe of array is denoted as A_{11}, the center element of array is marked as A_{36}, and A_{56} is placed in the midst of lowest row.

Active element radiation pattern is the pattern taken with a feed at the target element in the array, and with all other elements terminated in matched loads. Fig. 6 compares the active radiation

patterns of elements A_{11}, A_{36} and A_{56} with the pattern of a single antenna in the case of being isolated.

As expected, isolated element pattern and the active pattern of A_{36} are symmetric, but A_{36} has the relatively large backlobe due to the surface creeping wave. Fig. 6 (b) demonstrates that the given positions of A_{11} and A_{56} induce the unbalanced coupling effects on generating the contorted active element patterns. All the active element patterns will be imported into the formula (12), independently.

In particular, the HGA selection process in this paper will be used to choose the optimal excitation amplitude parameter for each of the elements, while maintaining a uniform phase distribution.

For generating a notched far-field pattern to restrain the interference coming from the special directions, the fitness function is defined as follow

$$\begin{aligned} Fitness = \quad & \omega_1 \cdot \left| 20 \cdot \log \left(\frac{1}{\phi_{SLL}} \sum_{\phi \in \phi_{SLL}} F(\theta_0, \phi) \right) - SLL \right|^2 \\ & + \omega_2 \cdot \left| 20 \cdot \log \left(\frac{1}{\phi_{NULL}} \sum_{\phi \in \phi_{NULL}} F(\theta_0, \phi) \right) - NULL \right|^2 \\ & + \omega_3 \cdot \left| 20 \cdot \log \left(\frac{1}{\phi_{NULL0}} \sum_{\phi \in \phi_{NULL0}} F(\theta_0, \phi) \right) - NULL0 \right|^2 \end{aligned} \tag{18}$$

where $F(\theta_0, \phi)$ is the far-field values calculated from (12), $\theta_0 = 90^\circ$ points the operational plane to the XY-plane, and ω_1, ω_2, ω_3 stand for the weight coefficients in the fitness function. SLL, $NULL$ and $NULL0$ represent given sidelobe level, goal notch depth and nulls depth, respectively.

5. OPTIMIZATION RESULTS

In the case of above antennas configuration and fitness function, we have synthesized two required notched patterns.

During the simulations, we adopted the following parameter suite:

- Population size: $pop = 150$;
- Crossover probability: $p_c = 0.75$;
- Mutation probability: $p_m = 0.15$;
- Maximum number of generations: $MaxG = 7000$.

When goal parameters $SLL = 20$ (dB), $NULL = 30$ (dB), $NULL0 = 50$ (dB), and notches domains are specified for pattern I,

ω_1, ω_2, ω_3 are given values of 0.32, 0.50 and 0.18 in the optimization, individually.

The optimized amplitudes of elements in the conformal antenna array are shown in the Table 1, and optimized radiation pattern I of array is demonstrated in Fig. 7.

Table 1. Optimized amplitudes of elements in the conformal array for pattern I.

	Row1	Row2	Row3	Row4	Row5
Column1	0.19893	0.28903	0.19634	0.30904	0.08315
Column2	0.2575	0.09603	0.29119	0.33146	0.26041
Column3	0.40702	0.69456	0.52570	0.67889	0.41017
Column4	0.69623	0.30242	0.64722	0.68869	0.50183
Column5	0.58224	0.30144	0.82765	0.56972	0.69997
Column6	0.37376	0.77449	0.85130	0.48461	0.39433
Column7	0.80030	0.69910	0.57073	0.53376	0.29530
Column8	0.79873	0.47374	0.31880	0.48160	0.78448
Column9	0.80478	0.77162	0.28498	0.23498	0.51974
Column10	0.09357	0.39085	0.23327	0.18269	0.20420
Column11	0.28557	0.09585	0.15827	0.40257	0.20615

Two deep notches, with the depth of 30 dB, are synthesized at the given angle domains of $-48 \sim -32$ deg and $29 \sim 46$ deg in the azimuthal plane. Angles at -46 deg, -34 deg, 32 deg and 44 deg have the specified nulls, with null depth below -50 dB. HGA also gives the -20 dB average sidelobe level for 5×11 conformal array.

The pattern obtained from normal Chebyshev amplitude distribution with $SLL = 20$ (dB) is also illustrated in Fig. 7. It is evident that normal Chebyshev amplitude distribution is no longer suitable to control the sidelobe level of conformal antenna array which has large curvature. Standard GA gets the similar optimized results, but not very ideal in controlling the sidelobe levels. Fig. 8 shows the converging line of HGA and GA, which demonstrates HGA procedure possesses the dominant speed and precision in the optimization compared with standard GA.

When changing notches angles and values of ω_1, ω_2, ω_3 to 0.26, 0.52, 0.22 respectively, we get radiation pattern II required in application which has notch in a large-domain in azimuthal plane shown in Fig. 9 excited by amplitude distribution in Table 2.

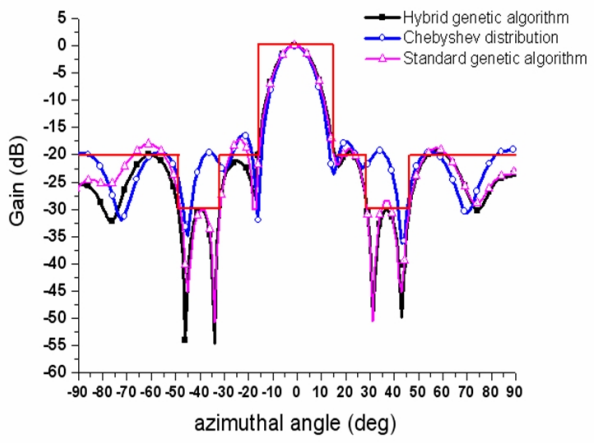

Figure 7. Notched radiation pattern I of conformal antenna array optimized by HGA.

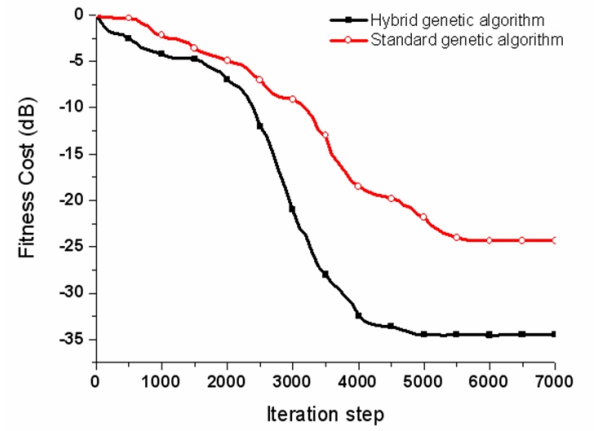

Figure 8. Comparison of iteration procedure between HGA and GA for pattern I.

In the comparison of large-domain notched pattern II between HGA and GA, the specified nulls at -33 deg and 45 deg are excursive with insufficient null depth in GA results. Fig. 10 demonstrates HGA possessing the steady optimization appearance contrasted with standard GA.

Table 2. Optimized amplitudes distribution of elements for generating notched pattern II.

	Row1	Row2	Row3	Row4	Row5
Column1	0.25994	0.067124	0.10036	0.33271	0.25637
Column2	0.30942	0.383250	0.12255	0.20253	0.10859
Column3	0.47757	0.735610	0.10384	0.31139	0.63008
Column4	0.71748	0.713860	0.30733	0.61421	0.97799
Column5	0.77083	0.254670	0.88380	0.68585	0.82878
Column6	0.76610	0.496740	0.98742	0.51862	0.83940
Column7	0.81694	0.804140	0.58378	0.75668	0.73385
Column8	0.97923	0.669310	0.76730	0.37445	0.79605
Column9	0.56448	0.645740	0.63780	0.29529	0.44072
Column10	0.3645	0.276990	0.35873	0.38221	0.40434
Column11	0.32282	0.25406	0.25488	0.42106	0.18754

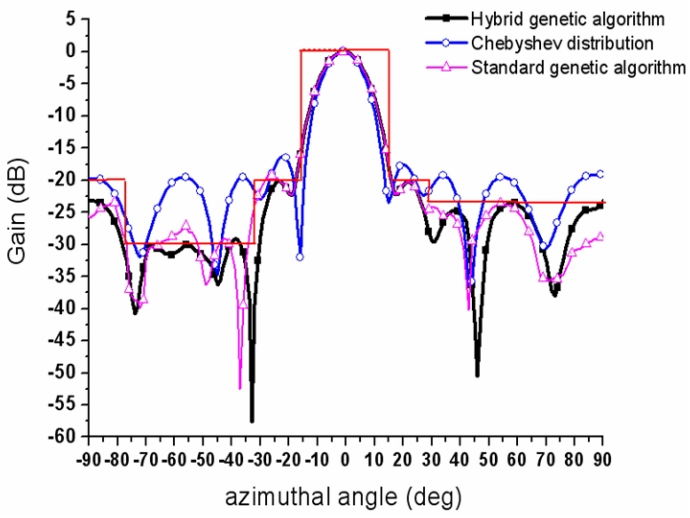

Figure 9. Notched radiation pattern II for conformal array optimized by HGA.

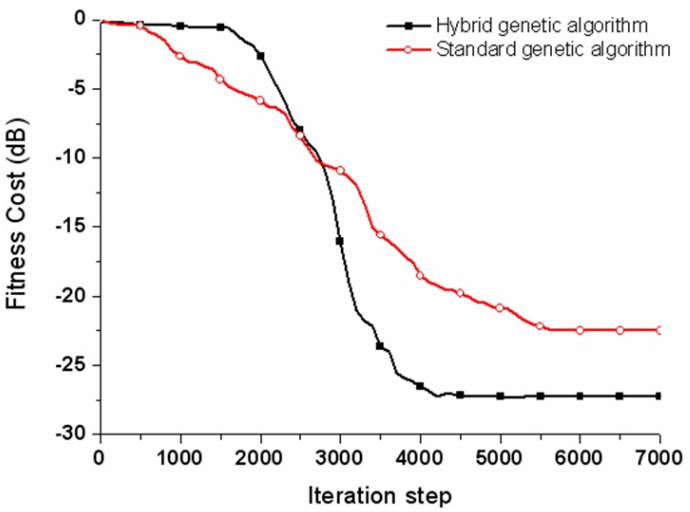

Figure 10. Contrast of iteration procedure for notched pattern II between HGA and GA.

6. CONCLUSION

This paper has demonstrated the application of the proposed hybrid genetic algorithm (HGA) to synthesize notched radiation pattern for a 5×11 conformal antenna array composed of multilayer patches antennas. Compared with standard GA, we find HGA could yield the optimal set of excitation current amplitudes in the precision accelerated converging process. Simultaneously, the effects of the mutual coupling on the radiation patterns can be compensated for using HGA procedure efficiently.

REFERENCES

1. Elliott, R. S., *Antenna Theory and Design*, Prentice-Hall, Englewood Cliffs, NJ, 1981.
2. Lo, Y. T. and S. W. Lee, *Antenna Handbook: Theory, Applications, and Design*, Van Nostrand, New York, 1998.
3. Mahanti, G. K., A. Chakraborty, and S. Das, "Design of fully digital controlled reconfigurable array antennas with fixed dynamic range ratio," *Journal of Electromagnetic Waves and Applications*, Vol. 21, No. 1, 97–106, 2007.

4. Babayigit, B., A. Akdagli, and K. Guney, "A clonal selection algorithm for null synthesizing of linear antenna arrays by amplitude control," *Journal of Electromagnetic Waves and Application*, Vol. 20, 1007–1020, 2006.
5. Lee, K. C. and J. Y. Jhang, "Application of particle swarm algorithm to the optimization of unequally spaced antenna arrays," *Journal of Electromagnetic Waves and Application*, Vol. 20, No. 14, 2001–2012, 2006.
6. Guney, K. and M. Onay, "Amplitude-only pattern nulling of linear antenna arrays with the use of bees algorithm," *Progress In Electromagnetics Research*, PIER 70, 21–36, 2007.
7. Mahanti, G. K., N. Pathak, and P. Mahanti, "Synthesis of thinned linear antenna arrays with fixed sidelobe level using realcoded genetic algorithm," *Progress In Electromagnetics Research*, PIER 75, 319–328, 2007.
8. Vaskelainen, L. I., "Constrained least-squares optimization in conformal array antenna synthesis," *IEEE Trans. Antennas and Propagation*, Vol. 55, No. 3, 859–867, 2007.
9. Kojima, N., K. Hariu, and I. Chiba, "Low sidelobe pattern synthesis using projection method with mutual coupling compensation," *IEEE International Symposium on Phased Array Systems and Technology*, 559–564, 2003.
10. Ferreira, J. A. and F. Ares, "Pattern synthesis of conformal arrays by the simulated annealing technique," *Electron. Lett.*, Vol. 33, No. 14, 1187–1189, 1997.
11. Ansell, D. W. and E. J. Hughes, "Using multi-objective genetic algorithms to optimise the subarray partitions of conformal array antennas," *Twelfth International Conference on Antennas and Propagation*, Vol. 1, No. 5, 151–155, 2003.
12. Boeringer, D. W., D. H. Werner, and D. W. Machuga, "A simultaneous parameter adaptation scheme for genetic algorithms with application to phased array synthesis," *IEEE Trans. Antennas and Propagation*, Vol. 53, No. 1, 356–371, 2005.
13. Li, H., Y. C. Jiao, and Y. Wang, "Integrating the simplified interpolation into the genetic algorithm for constrained optimization problems," *International Conference on Computational Intelligence and Security*, Part 1, LNAI 3801, 247–254, 2005.
14. Ali, M. M., A. Törn, and S. Vitanen, "A numerical comparison of some modified controlled random search algorithms," *Journal of Global Optimization*, Vol. 11, 377–385, 1997.